Achieving complete nitrification below the washout SRT with hybrid membrane aerated biofilm reactor (MABR) treating municipal wastewater

Santo Fabio Corsino[a]*, Michele Torregrossa[a]

[a] Department of Engineering, University of Palermo, Viale delle Scienze, 90128, Palermo, Italy

***Corresponding author: tel: +3909123861929; fax: +39 09123860810**

E-mail address: santofabio.corsino@unipa.it (Santo Fabio Corsino)

Abstract

This study analyzed the performances of a hybrid membrane aerated biofilm reactor (MABR) pilot plant in terms of nutrients removal of the attached growth and suspended biomass in comparison with a conventional activated sludge (CAS) system at different sludge retention time (SRT) (20-3) days. Overall, the MABR showed better performances than the CAS in terms of TSS (86% vs 79%), COD (89% vs 85%) and total nitrogen (80% vs 65%). The minimum SRT for achieving complete nitrification in the MABR was close to 3 days, corresponding to a SRT in the aerobic compartment of 1.9 days, whereas in the CAS it was equal to 8 days (aerobic SRT of 4.8 days). Nitrification rate in biofilm was on average equal to 0.40 gNH_4-N h^{-1} (2.40 gNH_4-N $m^{-2}d^{-1}$). Its contribution to the overall nitrification in the MABR plant was 25-30% on average, although it increased when the SRT was decreased.

Particle size distribution and microscopic analyses showed particles of biofilm detached from the membrane of the MABR. The seeding effect allowed sustaining nitrification of the suspend biomass at very low SRT. The nitrification rate observed in the suspended biomass in the MABR slightly decreased from 3.42 $mgNH_4$-N $gVSS^{-1}$ h^{-1} to 2.87 $mgNH_4$-N $gVSS^{-1}$ h^{-1} when the SRT was decreased from 20 days and 3 days, whereas in the CAS it collapsed from 2.33 $mgNH_4$-N $gVSS^{-1}$ h^{-1} to 0.47 $mgNH_4$-N $gVSS^{-1}$ h^{-1}, because of nitrifying washout. Moreover, the biofilm detachment involved a positive effect in settling properties of the suspended biomass.

Keywords: MABR; nitrogen removal; nitrification rate; settleability; washout SRT

List of abbreviations

AUR: Ammonium uptake rate

COD: Chemical oxygen demand

DO: Dissolved oxygen

DSVI: Diluted sludge volume index

EPS: Extracellular polymeric substances

IFAS: Integrated Fixed film Activated Sludge

LPM: Litre per minute

MABR: Membrane aerated biofilm reactor

MABR-AS: Membrane aerated biofilm reactor – Activated sludge

MLTSS: Mixed liquor total suspended solids

MLVSS: Mixed liquor volatile suspended solids

NLR: Nitrogen loading rate

NUR: Nitrate uptake rate

ORP: Oxidation reduction potential

OTE: Oxygen transfer efficiency

OTR: Oxygen transfer rate

NR: Nitrification rate

PSD: Particle size distribution

F/M: Food to microorganism ratio

SND: Simultaneous nitrification denitrification

SRT: Sludge retention time

TN: Total nitrogen

TP: Total phosphorous

TSS: Total suspended solids

WWTP: Wastewater treatment plant

1. Introduction

Membrane-aerated biofilm reactor (MABR) is emerging as a promising technology for the treatment of municipal and industrial wastewaters due its ability to degrade carbonaceous and nitrogenous pollutants simultaneously (Landes et al., 2021). MABR enables to achieve higher chemical oxygen demand (COD) and total nitrogen (TN) removal rates than conventional biofilm technologies, such as rotating biological contactors and biological aerated filters (Syron et al., 2015). Indeed, in the MABR technology a gas permeable membrane is employed to transfer oxygen to a biofilm growing on the surface of the membrane, whereas nutrients diffuse from the bulk into the biofilm according to a counter-diffusional mechanism. This means that oxygen is supplied to the inner part of the membranes, and it diffuses through biofilm toward the bulk, while substrates diffuse in the opposite direction. Thus, the most active zone is typically located in the interior of the biofilm (Nerenberg, 2016a). This leads to unique behavior and advantages over conventional biofilm system, like development of specialized microbial community, greater sensitivity to biofilm accumulation and lower susceptibility to liquid diffusion layer resistance (Nerenberg, 2016b). This diffusion mechanism allows for lower airflow rates and pressure, thus resulting in lower energy consumption. It was estimated in previous studies that this technology enables to save about 70% of aeration energy in comparison with fine bubble diffusers (Castrillo et al., 2019).

The above-mentioned advantages of MABR technology enabled to provide a more stable and efficient process for wastewater treatment, resulting a competitive solution to reduce the environmental and economic impacts of wastewater treatment plants (WWTP). Given the improvements of MABR technology in terms of process performances and stability, recently some researchers have incorporated MABR modules into anoxic zones of conventional activated sludge (CAS) plants for biological nutrients removal, resulting in the so-called hybrid configuration (Carlson et al., 2021; Uri-Carreño et al., 2021). Therefore, a hybrid MABR-activated sludge (MABR-AS) system is where the attached-growth MABR is coupled with a conventional suspended-growth process (Guglielmi et al., 2020). This solution could be very interesting for retrofitting of existing plants in which nitrification is the limiting step of nitrogen removal process, thereby providing additional nitrification capacity. Indeed, several recent studies have demonstrated that when used in a hybrid configuration with activated sludge, the MABR process can also improve treatment performances and intensify the overall treatment capacity of the WWTP (Bunse et al., 2020; Jeff Peeters et al., 2017).

Several researches on MABR have been carried out during the last decade, focusing on the advantage of the oxygen counter-diffusion mechanism to improve nitrogen removal or to achieve partial-nitrification and simultaneous nitrification-denitrification (SND) (Bunse et al., 2020; Zhang et al., 2021), as well as aimed at reducing energy requirements and greenhouse gases emissions (Kinh et al., 2017). Moreover, another advantage deriving from coupling biofilm and suspended biomass is the possibility to achieve complete nitrification at sludge retention time (SRT) lower compared with CAS system (washout SRT), since slowly growing nitrifying organism are retained in the biofilm and are not washed out with the suspended biomass (Ekama, 2015; Mannina et al., 2019).

Therefore, by using hybrid MABR technology it might be possible to reduce the design or operational SRT without losing the nitrification ability and thereby reducing the volume required for nitrification reactor or increasing the potentiality of a given one (Houweling et al., 2019).

Another benefit of coupling the MABR with conventional activated sludge processes could be the potential improvement of the suspended sludge settleability. Indeed, the biofilm detachment from membrane might improve the settling properties of suspended biomass in hybrid MABR system because of the flocculation capacity of the biofilm (Hu et al., 2017). This phenomena, also called “seeding effect”, could be beneficial especially in those WWTP in which filamentous bulking phenomena occur chronically (Jenkins et al., 2003). However, there are no studies yet that explored the possible improvement of the sludge settleability in MABR hybrid configuration resulting from the interaction between suspended and attached-growth bacteria.

Although recent developments, operational performance, kinetic parameters of both biofilm and suspended biomass in hybrid MABR systems are limited to mathematical modelling or laboratory scale plants (Carlson et al., 2021; Zhang et al., 2021), whereas full-scale or pilot-size installations are still very scarce (Nerenberg, 2016b). Moreover, the benefits of the seeding effect for enabling nitrification at SRT below the washout SRT of CAS should be validated.

This study presents the results obtained in a hybrid MABR pilot plant fed with real wastewater. The aims of the study were to assess the overall performances of the MABR in comparison with an identical conventional activated sludge (CAS) plant operating at SRT decreasing from 20 days to 3 days. More precisely, the study aimed to provide insights into nitrification kinetics of the biofilm and suspended biomass ad different SRT and, lastly, to evaluate possible mutual advantages arising from the interaction between biofilm and suspended biomass in terms of settling properties of the suspended activated sludge.

2. Materials and methods

2.1 Pilot plant description

The experimental campaign was carried out in a pilot plant consisting into two identical process lines working in parallel realized at the Palermo's wastewater treatment plant (Acqua dei Corsari). The pilot plant layout is reported in Figure 1.

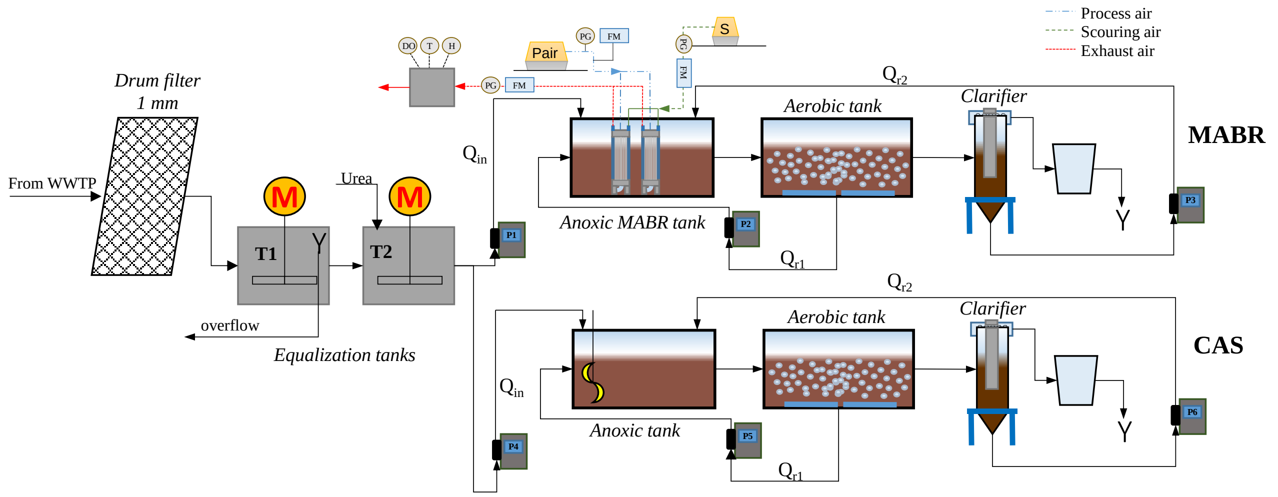

Figure 1: Pilot plant layout

The raw wastewater was continuously collected downstream of the preliminary treatment units of the main WWTP (after the screening and grit removal unit) and the fed in a stirred equalization unit, consisting of two tanks (40 L of volume each) connected in series, after being sieved in a rotating drum screen (mesh opening 1 mm, courtesy of Saveco). In the first tank (T1), the raw wastewater was only stirred to avoid solids separation and the excess flow was discharged to limit the influent flow to the pilot plant. The second tank (T2) was hydraulically connected to the first one and it was continuously stirred as well. From this tank, the wastewater was fed to the pilot plants by means of two dedicated peristaltic pumps with a flow rate of 40 L h^{-1} each.

Each of these process lines were realized according to a pre-denitrification scheme, consisting of one anoxic reactor (105 L) followed by one aerobic (160 L) and a vertical-flow clarifier (50 L). In the first process line, named MABR, 16 ZeeLung modules (courtesy of Suez) were installed in the anoxic reactor. Each membrane module accounts for 0.25 m^2 of media available for biofilm growth, thereby resulting in an overall media surface of 4 m^2. Each module is formed by cords. The cord structure consists of a braided polyester support, surrounded by a number of filaments (lumens). Each lumen is coated with a dense gas-permeable membrane. Air, at pressure higher than the hydrostatic pressure of the water level, is supplied to the module top header. The air passes inside of the lumens and oxygen diffuses through the membrane where it is consumed by bacteria that have formed a biofilm on the outer wall of the lumen. The braided polyester structure of the cord makes it virtually unbreakable and suitable for installation in activated sludge (Guglielmi et al., 2020). The membrane modules were connected to two dedicated air compressors that provided for the supply of air for process and scouring.

In the second process line, named CAS, the anoxic reactor was equipped with a vertical-axis mixer to ensure complete mixing.

The aerobic reactors were identical for the two lines. Each of them was equipped with a dedicated blower connected with two fine bubbles diffusers that provided air continuously. From the aerobic reactors, the mixed liquor was pumped to the anoxic tank via an internal recycling characterized by a flow rate equal to 100±10 L h^{-1} (Q_{r1}).

The mixed liquor passed from the aerobic reactor to the final clarifier, from which a constant flow (40 L h^{-1}) of settled sludge was recirculated to the anoxic reactor of each plant (Q_{r2}), whereas the clarified effluent was accumulated into two storage tanks (50 L of volume) and then discharged.

2.2 Experimental set-up, monitoring and operation

The pilot plant was operated for 304 days divided into four experimental periods, named Period 1 (229 days), Period 2 (33 days), Period 3 (25 days) and Period 4 (17 days), characterized by different SRT to compare the minimum SRT required for achieving biological nitrogen removal in a hybrid MABR and CAS plant. More precisely, in Period 1, the SRT was set to 20 days, whereas it was decreased to 8 days, 6 days and 3 days in Period 2, Period 3 and Period 4 respectively. More precisely, the SRT in the aerobic compartment, from now called aerobic SRT, of both the process lines was equal to 12 days (Period 1), 4.83 days (Period 2), 3.62 days (Period 3) and 1.8 days (Period 4). The SRT was controlled by purging a known volume of mixed liquor from the aerobic tank of each line daily and taking into account the amount of TSS withdrawn with the effluent. The SRT for each process line was calculated according to the equation 1:

$$\mathrm{SRT} = \frac{\mathrm{X_{TSS}}(\mathrm{g\ TSS\ L^{-1}}) \cdot \mathrm{V_{reactor}}\ (\mathrm{L})}{\mathrm{X_{aer,TSS}}\ (\mathrm{g\ TSS\ L^{-1}}) \cdot \mathrm{V_{wasted-sludge}}(\mathrm{L\ d^{-1}}) +\ \mathrm{X_{TSS-effluent}}(\mathrm{g\ TSS\ L^{-1}}) \cdot \mathrm{V_{discharge}}\ (\mathrm{L\ d^{-1}}\ )} \qquad (1)$$

Where the X_{TSS} is the average TSS concentration in the aerobic and anoxic compartments in g TSS L-1, $V_{reactor}$ is the sum of the anoxic and aerobic volume (265 L), $X_{aer,TSS}$ is the average TSS concentration in the aerobic compartment, $V_{wasted\text{-}sludge}$ is the volume of mixed liquor withdraw per day (L d^{-1}) from the aerobic tank, including also samples for analytical measures, $X_{TSS\text{-}effluent}$ is the concentration of solids in the effluent (g TSS L^{-1}) and $V_{discharge}$ is the volume of effluent discharged per day.

Because the raw wastewater lacked in nitrogen and soluble organic carbon, a concentrated solution containing urea from Period 1 and urea and sucrose from Period 2, was dosed in T2 with a constant flow of 1 L/h. Table 1 summarized the main features of the wastewater in the four experimental periods.

Table 1: Average characteristics of the influent wastewater during the experiment

Parameter	**Unit**	**Period 1**	**Period 2**	**Period 3**	**Period 4**
COD	mg L^{-1}	288±34	713±65	833.5±45	611.5±45
BOD_5	mg L^{-1}	125±32	441±36	520.5±36	443.3±36
NH_4-N	mg L^{-1}	33.6±2.7	32.1±8.7	37.1±8.7	36.7±8.7
NO_3-N	mg L^{-1}	0.57±0.01	1.27±0.39	1.9±0.39	0.7±0.39
NO_2-N	mg L^{-1}	0.06±0.01	0.30±0.08	0.03±0.08	0.01±0.08
TN	mg L^{-1}	42±3.6	48±13.3	59.4±13.3	60.5±13.3
PO_4-P	mg L^{-1}	1.44±1.0	2.30±0.72	2.16±0.72	1.21±0.72
TP	mg L^{-1}	3.12±1.64	3.20±0.54	3.54±0.54	2.68±0.54
TSS	mg L^{-1}	164.9±174	462±60	999±60	582±60
Conductivity	µS cm^{-1}	3040±40	2280±663	3280±663	4040±663
Chloride	mg L^{-1}	1080.5±54	993.3±234	1251.8±234	1687.9±234

The overall flow rate of process air delivered to the membrane modules in the MABR ranged between 37-44 NL h^{-1} (2.625 NL h^{-1}module^{-1}, 10.5 NL $h^{-1}m^{-2}$ on average). The pressure value at the air inlet of the membranes was approximately 0.4-0.5 bar, whereas the outlet pressure was between 0.20-0.35 bar. The exhaust air was collected from all the 16 membranes and sent to a digital flow meter that registered the exhaust flow rate continuously and from this to a tight-fitting box in which a sensor for measuring oxygen concentration was installed. Then, the exhaust air was expelled into the atmosphere. Air scouring was provided with a flow rate of 2.5 NL h^{-1}module^{-1} (10 NL $h^{-1}m^{-2}$) at a pressure of 0.18 bar. More precisely, the scouring air was supplied to a membrane pair intermittently, according to an operational cycle consisting of 10 seconds on, 70 seconds off. To avoid sludge settling in the anoxic reactor, a supplementary mixing system was installed. It consisted in two submerged mixers placed at opposite corners of the tank.

A constant airflow rate of 20 liters per minutes (LPM) was delivered to the aerobic reactors in the MABR and CAS, to maintain the dissolved oxygen at a concentration of approximately 5.0±0.5 mg L^{-1}.

The pilot plant was inoculated with activated sludge collected from the RAS line of the main WWTP. The mixed liquor total suspended solids (MLTSS) concentration of the seed sludge was approximately 8 gTSS L^{-1}, thus it was diluted with tap water to achieve a concentration close to 3 gTSS L^{-1}.

The pilot plant was equipped with online sensors (NH_4-N, NO_3-N, MLTSS) placed in different sections (influent tank, anoxic, aerobic reactors) and connected to a control unit (WTW IQ Sensor Net System 2020 XT). Moreover, digital flow meters, pressure gauges, oxygen, humidity and temperature sensors were installed in the process and exhaust air lines. A summary of the main process parameters and the membrane characteristics and operation are reported in Table 2.

Table 2: Summary of the main operating parameters in different sections of the MABR and CAS plant and ZeeLung membrane characteristics and operation

	Influent	**MABR**		**CAS**	
	T2	**Anoxic**	**Aerobic**	**Anoxic**	**Aerobic**
DO [mg L^{-1}]	n.m.	0.07±0.11	5.51±1.85	0.02±0.01	5.03±0.78
ORP [mV]	-200±0.03	10±7	142±21	-40±16	136±15
pH [-]	7.2±0.06	7.2±0.09	7.1±0.05	7.2±0.08	7.1±0.06
T [°C]	19±5.2	19±4.3	19±3.1	19±3.8	19±3.6
TSS [mg L^{-1}]	340±336	2730±320		3320±235	
VSS [mg L^{-1}]	n.m.	2219±185		2682±191	
F/M [kgBOD $kgTSS^{-1}d^{-1}$]*	-	0. 29±0.22		0.27±0.17	
ZeeLung membrane characteristics and operation					
Membrane surface [m^2]	4				
Process air flow/pressure [NL h^{-1}/bar]	42/0.4-0.5				
Exhaust air flow/pressure [NL h^{-1}/bar]	18/0.2-0.35				
Scouring air flow/pressure [NL h^{-1}/bar]	40/0.18				

n.m.: not measured
* Average value during the four experimental periods

2.3 Analytical methods

All the physical-chemical analyses, including TSS, VSS, COD, TN, TP, NH_4-N, NO_3-N, NO_2-N and PO_4-P, performed in the biological reactors, in the influent and effluent wastewater, as well as in the supernatant of the mixed liquor were measured according to standard methods (APHA, 2005).

Total Kjeldahl Nitrogen (TKN) was calculated through mass balances, by subtracting the concentrations of nitrite and nitrate in a specific sampling section to that of the TN. Furthermore, the main process parameters, including dissolved oxygen (DO), oxidation reduction potential (ORP) and pH were daily monitored in the T2 and the biological reactors by means of specific probes connected to a multimeter (WTW 3420).

The settling properties of the activated sludge were evaluated by means of the diluted sludge volume index ($DSVI_{30}$). Specifically, on each analytical day, settling tests were performed with samples having different TSS concentration, obtained by diluting the sample collected from the aerobic reactor with well clarified wastewater, according to the diluted sludge volume index (DSVI) procedure (Jenkins et al., 2003). More precisely, three of two-fold dilutions of the mixed liquor (n=0, no dilution, n=1, 1:1 dilution, n=2, 1:3 dilution) were performed in a 1 L graduate cylinder, until achieving a final settled volume lower than 200 mL. Microscopic observations were carried out for the analysis of the flocs morphology and the identification of filamentous bacteria. Observations were performed under phase contrast at 100× and 1000× magnifications. The filamentous microorganisms were morphologically identified using the Eikelboom classification system, whereas the abundance and dominance were estimated according to the literature (Jenkins et al., 2003).

The average size of the activated sludge flocs was analysed by means of a high-speed image analyses sensor (Sympatec Qicpic) that produced the particle size distribution (PSD) of the particles.

Finally, the extracellular polymeric (EPS) content of the sludge was determined according to the literature (Corsino et al., 2020)

2.4 AUR tests in biofilm and suspended biomass

To evaluate the nitrogen removal kinetics of the biofilm and suspended biomass, ammonium utilization rate (AUR) tests were performed during each of the experimental periods. The tests on the biofilm were performed by placing two membrane modules within a 30 L batch reactor filled with tap water. The membranes were connected to the process and scouring air lines, to reproduce the same operating conditions of the anoxic reactor except the presence of the suspended biomass. Ammonium chloride was supplied to achieve an initial ammonium-nitrogen concentration of approximately 40 mg NH_4-N L^{-1} to avoid substrate limitation during the test.

The AUR tests on the suspended biomass were performed in a 1.5 L batch reactor (2.5-3 gTSS L^{-1}) at room temperature. Six tests, two for each experimental period, were performed during the experiment. Ammonium chloride was added as ammonia source (initial ammonium-nitrogen concentration equal to 40 mg NH_4-N L^{-1}) during AUR tests. DO was provided via a fine bubble diffuser and it was maintained close to the saturation value.

AUR tests for both the biofilm and the suspended biomass were operated for 4 hours each, during which 20 mL of sample was withdrawn at regular time intervals (20 minutes), filtered through a 0.45 µm membrane and stored at 4°C for NH_4-N, NO_2-N and NO_3-N analyses.

The nitrification rate of the biofilm was calculated as the slope of the linear regression line of NH_4-N data and then referred to the membrane modules surface (0.5 m^2) and 20 °C by applying the Arrhenius equation (θ=1.07). The occurrence of simultaneous nitrification-denitrification was evaluated as the difference between the slope of ammonium consumed and nitrate produced (no nitrite accumulation was observed in any trials). Similarly, the AUR for the suspended biomass was calculated as the slope of the linear regression line of NH_4-N and then referred to the VSS concentration and 20 °C by applying the Arrhenius equation (θ=1.07).

2.5 Kinetic parameters of the suspended autotrophic biomass

The autotrophic biomass kinetic parameters were evaluated in the suspended biomass of both the MABR and CAS at the end of each period, once steady state was reached. The maximum growth rate ($\mu_{max,N}$), the endogenous decay rate (b_N) and the active fraction (f_{XN}) were evaluated at standard temperature (20 °C) by means of respirometric techniques according to previous literature (Capodici et al., 2016). Based on the above parameters, the minimum aerobic SRT to achieve a target effluent ammonia concentration was calculated assuming steady state conditions using the equation 2 (Metcalf & Eddy, 2014):

$$SRT = \frac{1}{\left[\mu_{max,N} \cdot \left(\frac{N}{k_N + N}\right)\left(\frac{DO}{k_{DO} + DO}\right) - b_N\right]} \qquad (2)$$

where:

$\mu_{max,N}$: the maximum specific growth rate of nitrifying organisms, d^{-1};

N: the effluent ammonia nitrogen concentration, equal to 2 $mgNH_4$-N L^{-1};

K_N: the half saturation for ammonia nitrogen, equal to 1 $mgNH_4$-N L^{-1};

DO: the dissolved oxygen concentration, equal to 5 mgO_2 L^{-1};

K_{DO}: the half saturation for dissolved oxygen, equal to 1 mgO_2 L^{-1};

b_N: the endogenous decay rate of nitrifying organisms, d^{-1}.

2.6 Oxygen transfer indicators

The oxygen transfer indicators for MABR technology were considered the oxygen transfer efficiency (OTE) and the oxygen transfer rate (OTR). The OTE and OTR were calculated according to the equation 3 and equation 4 respectively:

$$OTE = \frac{20.9\% - O_2\%_{exhaust\ air} \cdot \frac{1 - 20.9\%}{1 - O_2\%_{exhaust\ air}}}{20.9\%} \qquad (3)$$

$$OTR\ \left(\frac{gO_2}{m^2 \cdot d}\right) = \frac{OTE \cdot Q_{air}\left(\frac{L_{air}}{h}\right) \cdot 20.9\%\left(\frac{molO_2}{mol_{air}}\right) \cdot 32\left(\frac{gO_2}{molO_2}\right) \cdot 24\left(\frac{h}{d}\right)}{22.4\left(\frac{L}{molO_{air}}\right) \cdot A_{biofilm}(m^2)} \qquad (4)$$

The Q_{air} in equation 4 was process air flow rate at the inlet of the modules, the area of biofilm was assumed equal to the overall surface of the membranes (4 m^2), whereas all the other parameters were continuously measured by the sensors.

2.6 Mass balances and calculations

Overall removal performances for TSS, COD, TN, NH_4-N were calculated according to the equation 5:

$$\eta = \frac{C_{in} - C_{out}}{C_{in}} \cdot 100 \quad (5)$$

Nitrification rate (NR) of the biofilm was calculated by a mass balance for total Kjeldahl nitrogen (TKN) performed in the anoxic reactor of the MABR line according to the following equation 6:

$$NR = \frac{Q_{in} \cdot TKN_{in} + Q_{r2} \cdot TKN_{out} + Q_{r1} \cdot TKN_{aerobic} - (Q_{in} + Q_{r2} + Q_{r1}) \cdot TKN_{anoxic} - N_{synthesis}}{1000} \quad (6)$$

in which TKN_{in}, TKN_{out}, $TKN_{aerobic}$, TKN_{anoxic} were the TKN concentration in the influent and the effluent wastewater and in the supernatant of the aerobic and anoxic reactor, respectively, whereas $N_{synthesis}$ was the ammonium removed for heterotrophic synthesis, calculated based on the COD removed in the anoxic compartment. The latter was measured by performing batch tests in which the ammonium nitrogen consumption was determined after inhibition of the ammonium oxidizing bacteria through the addition of allylthiourea. Overall, the ammonium nitrogen removed by heterotrophic synthesis was on average equal to 3.0% of the removed COD in the MABR and CAS. For the statistical analysis, the t-test was applied (MS Excel tool) to evaluate the significance of differences kinetics and characteristics between sludges. The significance level of probability (p-value) was 0.01 in this study.

3. Results and discussion

3.1 Pilot plant performance

The analytical measurements enabled to assess the pilot plant performances throughout the entire experiment. The trends of the TSS, COD, TN, NH_4-N, NO_3-N, NO_2-N in the influent and the effluent of the pilot plant, as well as the removal efficiencies, are depicted in Figure 2.

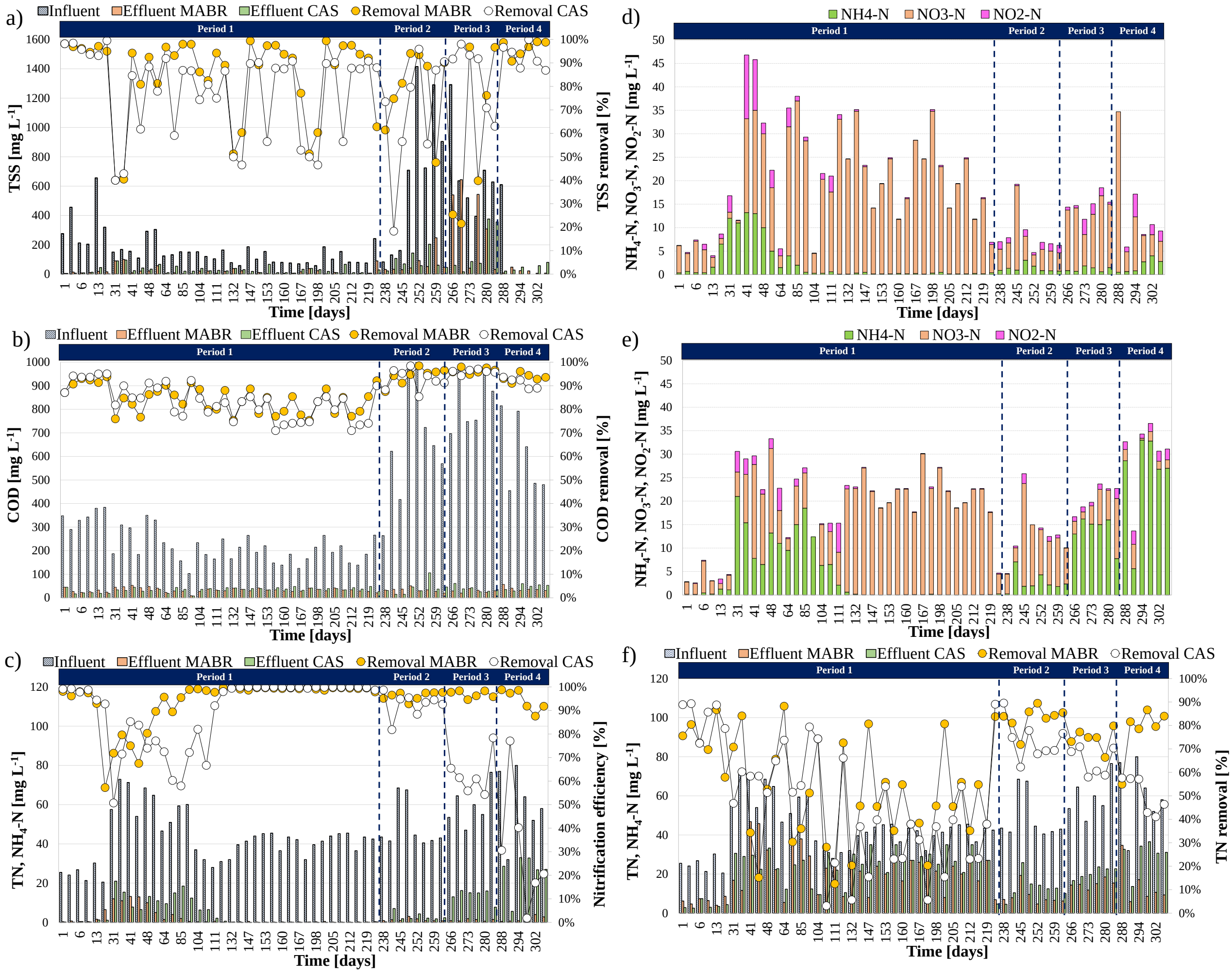

Figure 2: Influent, effluent concentrations and removal efficiencies of TSS (a) and COD (b); influent TN and effluent concentration of ammonium and nitrification efficiency (c); effluent concentration of nitrogen ionic species (NH_4-N, NO_2-N, NO_3-N) in the MABR (d) and CAS (e); influent, effluent concentrations and removal efficiency of TN in the MABR and CAS (f).

The TSS concentration of the raw wastewater was variable during the entire experiment according to climate conditions that affected the amount of grit in the sewage (Fig. 2a). The effluent concentration of TSS significantly fluctuated in both the lines during the four periods and in some days it exceeded the discharge limit imposed by European regulations (35 mg L^{-1}) in both the MABR and CAS.

Overall, the average effluent concentration during the entire experiment was equal to 52 mg L^{-1} and 83 mg L^{-1} in the MABR and CAS, respectively, thereby indicating a better solids retention capacity of the MABR compared with the CAS. According to what above, the removal performances significantly fluctuated between 40-99% in both the lines, depending on the influent TSS concentration. Overall, the MABR performed better removal efficiency of TSS resulting close to 86% on average, whereas the CAS exhibited a lower removal capacity of solids (78%). The exceedance of TSS in the effluent of both the line was due to the occurrence of rising in the final clarifiers. This phenomenon determined the rise of the settled sludge to the surface as a result of denitrification process in the clarifier's hopper. Rising sludge was more evident in the CAS line because of the higher nitrate concentration as will be better discussed in the following. This determined a TSS concentration in the effluent of the CAS higher than the MABR, on average.

Figure 2b shows the influent concentration of the COD and that in the supernatant of the aerobic tanks, as well as the removal performances obtained in the MABR and CAS. The influent COD concentration ranged between 100-990 mg L^{-1} during the experiment. It is worth noticing that in Period 1, the average COD concentration was close to 200 mg L^{-1}, thus substantially lower compared with a typical municipal wastewater. This was likely due to the infiltration of marine water eddy in the sewage network as suggested by the high amount of chloride and conductivity observed during the entire experiment (Table 1). Nonetheless, both the MABR and the CAS achieved high removal performances of the organic carbon. The COD concentrations in the supernatant of the aerobic tank of both the process lines were below 30 mg L^{-1} during the entire Period 1. More precisely, the average COD concentration in the MABR was equal to 24 mg L^{-1}, whereas in the CAS it was 28 mg L^{-1}, thereby resulting in a removal efficiency of approximately 89% and 86% in the MABR and CAS, respectively. In the following periods (Period 2, Period 3 and Period 4), the influent COD concentration increased to approximately 700 mg L^{-1} on average, because of the supply of an external carbon source to enhance denitrification process. The average COD concentration in the supernatant of the MABR was close to 35 mg L^{-1}, whereas in the CAS it was equal to 52 mg L^{-1}, resulting in removal efficiencies equal to 95% and 89% in the MABR and CAS, respectively. Even regarding the COD removal, the MABR showed a slightly higher performance compared to the CAS. Moreover, it is worth noticing that COD removal in the MABR was more stable, showing overall a more limited variation in performance compared with the CAS and no significant relationship with the SRT were noted in both the lines. This result demonstrated that the MABR was able to reduce the effects of the change in wastewater composition on the suspended biomass, thereby making the overall hybrid system more resilient to influent streams that have variable COD concentrations.

The time courses of the TN concentration in the influent and the effluent ammonium concentrations and nitrification performances achieved in the MABR and CAS are depicted in Fig. 2c. The ammonium removal significantly fluctuated during the first stage of Period 1 in both the MABR and the CAS, likely because of the increase of the TN concentration in the influent wastewater from the 30th day given the supply of urea in the feeding tank (T2). Nevertheless, complete nitrification was obtained after 98 days in the MABR and 128 days in the CAS, thereby indicating that the MABR showed a more rapid tendency to reach steady state with respect to the CAS. Stable nitrification efficiency close to 99% was observed in both the lines until the end of Period 1, resulting in an effluent ammonium concentration lower than 1 $mgNH_4$-N L^{-1}. When the SRT was decreased to 8 days in Period 2, the ammonium removal efficiency did not change in the MABR, whereas at steady state in the CAS it decreased to approximately 93%, resulting in an effluent ammonium concentration in the effluent close to 2 $mgNH_4$-N L^{-1}. Similarly, the further decrease of the SRT to 6 days in Period 3 caused a significant reduction of the nitrification efficiency in the CAS. Indeed, the effluent ammonium concentration at steady state increased to 12 $mgNH_4$-N L^{-1} and accordingly the nitrification efficiency decreased to 60% on average. In contrast, no significant changes were noted in the MABR, in which the effluent ammonium concentration was always below 1 $mgNH_4$-N L^{-1} and the nitrification efficiency was stable at 97-98%. Finally, in Period 4, nitrification efficiency collapsed to less than 25% in the CAS, thereby resulting in an effluent ammonium concentration close to 30 $mgNH_4$-N L^{-1}, on average. In the MABR, nitrification efficiency slightly decreased only at the end of Period 4, although the ammonium removal resulted higher than 93% and the effluent ammonium concentration was close to 2 $mgNH_4$-N L^{-1}. The above results suggested that the operating conditions imposed in the CAS caused the washout of the nitrifying biomass, thereby causing the accumulation of ammonium in the effluent. The minimum value of the SRT that enabled to obtain high nitrification performance in the CAS was 8 days, whereas lower values caused a significant loss in nitrification capacity of the system. In contrast, the MABR enabled very high nitrification efficiency up to 3 days of SRT, thereby showing a higher nitrification capacity respect the conventional line even below the washout SRT.

The nitrogen species in the effluents of the MABR and CAS changed according to the SRT (Fig. 2d and Fig. 2e). Specifically, at steady state in Period 1 nitrate accounted for approximately 99% in both the MABR and the CAS, whereas the percentages of ammonium and nitrite were negligible. The effluent nitrate concentrations were close to 20 mg L^{-1} on average, suggesting a limitation in denitrification process in both the lines. Indeed, the amount of readily biodegradable COD in the raw wastewater was very low in Period 1, resulting in a BOD/NO_3-N ratio lower than 3, thus not sufficient to achieve high denitrification rates. In Period 2, nitrate was still the main nitrogen specie in the effluents of the MABR and CAS, although the ammonium concentration increased in the CAS because of the decrease of nitrification efficiency. Moreover, the effluent nitrate concentration decreased compared to Period 1, because of the supply of the external carbon source that improved denitrification efficiency in both the lines. It was worth noticing that a slight nitrite accumulation started to be observed in the effluent of both the MABR and CAS in Period 2 because of the increase in the chloride concentration of the raw wastewater that caused a partial inhibition of the nitrite oxidizer bacteria (Pronk et al., 2014). In Period 3, the main nitrogen specie in the effluent of the CAS was the ammonium, accounting for about 74%, because of the loss in nitrification capacity, whereas nitrate accounted for more than 90% of the total nitrogen in effluent of the MABR. Lastly, in Period 4 the effluent ammonium concentration slightly increased in the MABR and that of nitrate decreased accordingly, thus accounting for approximately 30% and 45% of the effluent TN, respectively. In the

CAS, the percentage of ammonium in the effluent further increased respect to Period 3, accounting for more than 95%.

Figure 2f depicts the trends of the influent and effluent TN concentrations in the MABR and CAS, as well as the removal efficiencies obtained during the experiment. In Period 1, the effluent TN concentration significantly fluctuated in both the MABR and CAS. Indeed, the effluent concentrations and removal efficiencies in both the lines were on average close to 24 mgTN L^{-1} and 45%. As above discussed, in Period 1 TN removal performance was affected by limitation in denitrification in both the process lines. Indeed, when the external carbon source was supplied from Period 2, TN removal significantly improved, resulting close to 85% and 76% in the MABR and CAS, respectively. In Period 3, TN removal was quite similar compared to the previous period in the MABR (81% on average), whereas it slightly decreased in the CAS to 60% because of loss in nitrification performance. Finally, in Period 4, TN removal still decreased in the CAS to less than 40% and it was reasonable to speculate that nitrogen was removed by heterotrophic assimilation. In contrast, TN removal close to 85% was still achieved in the MABR, thereby confirming that stable nitrification-denitrification could be achieved in hybrid MABR system at SRT lower than washout SRT of the CAS.

The results above suggested that overall, the MABR showed a significantly higher nitrification capacity compared to the CAS with the decrease of the SRT. The short SRT caused in the CAS a significant washout of nitrifying bacteria that involved a gradual accumulation of ammonium in the effluent because of the loss in nitrification capacity. Conversely, this was not observed in the MABR that enabled very high nitrification efficiency and nitrogen removal even at SRT of 3 days. Certainly, the biofilm contributed to the higher nitrification obtained in the MABR (see paragraph 3.2), but the higher performances achieved in the MABR suggested that the biofilm detachment from the membrane acted as a continuous source of inoculum of nitrifying bacteria for the suspended sludge, thereby enabling to sustain nitrification even at SRT much lower than the conventional system.

Moreover, the MABR enabled a higher resilience toward the variation of the nitrogen load in the influent wastewater, thereby resulting in more stable performances under varying operating conditions.

3.2 Insight into nitrification in the MABR

To provide insight into nitrification in the MABR, mass balances were performed with the aim to evaluate the ammonium removed the biofilm and its contribution to the overall nitrification performance.

Figure 3 depicts the time courses of the overall TKN removed in the MABR and the one removed in the anoxic compartment only.

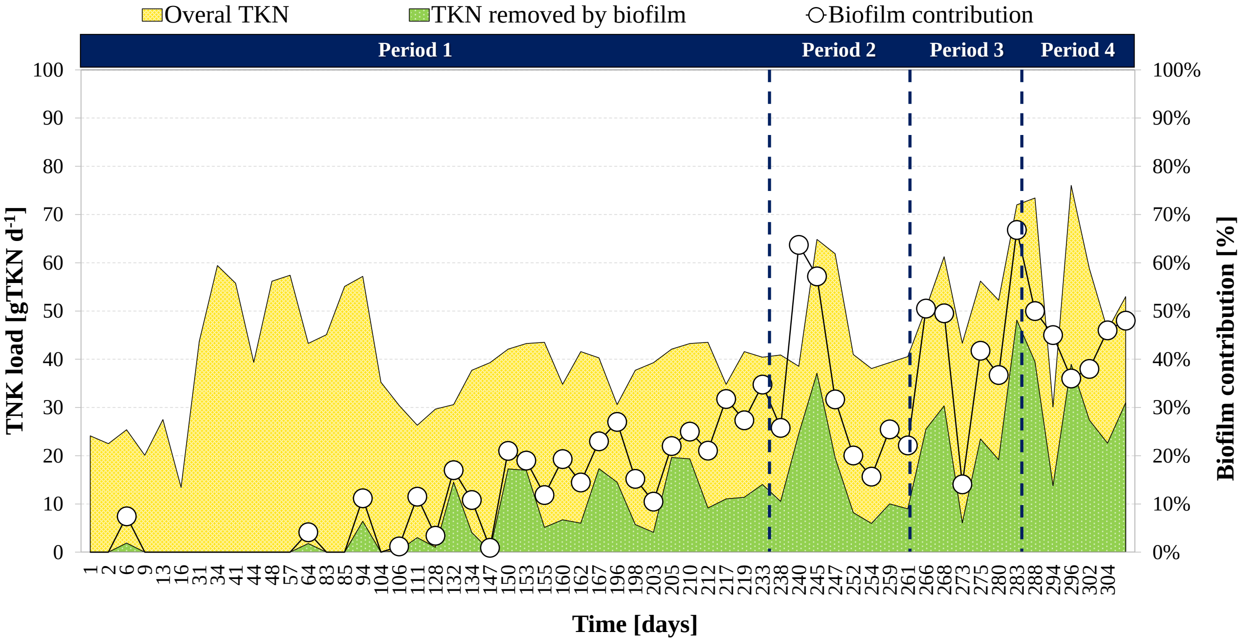

Figure 3: Trends of the overall TKN removed in the MABR (yellow curve), in the anoxic compartment by the biofilm (green curve) and the percentage contribution of the biofilm to the TKN removed (white dots).

During the early stage in Period 1, the occurrence of nitrification in the biofilm was negligible. Indeed, the influent TKN load was mainly removed by nitrification in the aerobic reactor. Nitrification by the biofilm was observed from the 94th day and it gradually increased during Period 1, although a stable rate was observed only after the 150th day, indicating that biofilm reached its maturation after this day. At steady state, the ammonium removal rate in the biofilm was close to 9.60 gTKN d^{-1} (2.40 gTKN $m^{-2}d^{-1}$) on average, accounting for approximately 25% of the overall TKN removed, although the trend was quite variable and related to the influent ammonium load variation. From Period 2 onward, the TKN removed by the biofilm increased although showing a fluctuating tendency, reaching a value of approximately 25 gTKN d^{-1} (6.25 gTKN $m^{-2}d^{-1}$) at the end of Period 4, also due to the increase of the temperature up to 27 °C (Fig. S1).

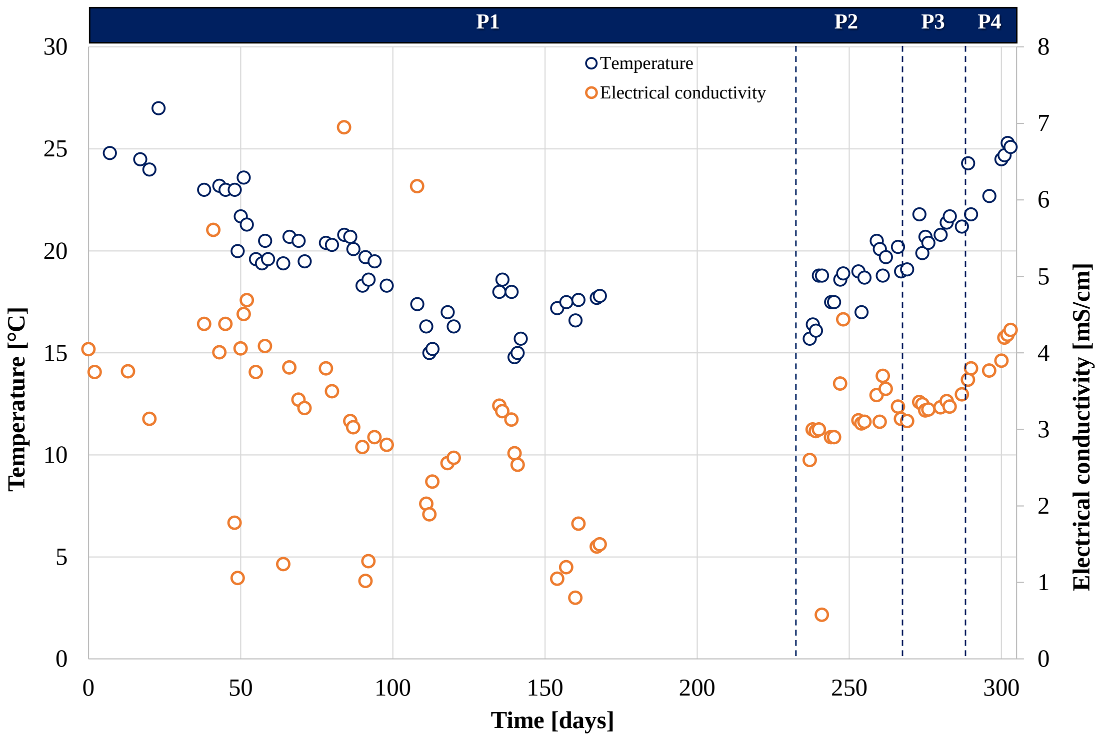

Figure S1: Trends of temperature and electrical conductivity during the experiment

Accordingly, the contribution of the biofilm to the overall TKN removal increased to approximately 45% at the end of the experiment. These results suggested that the biofilm contribution to nitrification increased as the SRT decreased. Therefore, the loss in nitrification efficiency caused by the washout of nitrifying in the suspended biomass was compensated by the nitrification capacity of the biofilm.

Consequently, MABR enabled to cope with shorter SRT compared to conventional activated sludge systems thanks to the increase of nitrifying biomass developing on the membrane fibers and that was not affected by the washout that involved the suspended biomass only.

Furthermore, the results above indicated a certain variability of the TKN removal rate by the biofilm. A possible explanation to this result could be the variation of the biofilm thickness. Indeed, it was demonstrated that the thickness of the biofilm affects the ammonium removal and nitrification kinetic (Matsumoto et al., 2007). Moreover, as reported in previous studies, the thickness of biofilm is determined by the balance of growth and detachment processes (Horn et al., 2003). The maintenance of a stable thickness of biofilm is not easy to achieve because it is affected by a combination of processes, including abrasion, erosion, sloughing and predator grazing which are difficult to manage (Bryers, 2018). Consequently, it is possible that the thickness of the biofilm was not constant during the experiment. As will be better elucidated in the following sections, biofilm detachment from the membranes was not constant during the experiment and it is reasonable to speculate that the biofilm thickness changed according to a dynamic process involving bacterial growth and detachment phenomena. Nevertheless, biofilm enabled to maintain a minimum nitrification rate, thus contributing in any case to the ammonium oxidation.

Moreover, it is worth noticing that biofilm started to develop only after approximately 60 operating days and a complete maturation was observed close the 150th day. Compared with previous literature, the biofilm formation and maturation process were slower. Indeed, Peeters and coauthors obtained steady state performances after approximately 30 days (Peeters, 2016), whereas Wang et al. achieved a fast start-up of two MABRs at different NRL, low and high, in 23 and 33 days, respectively (Wang et al., 2019). Similarly, the startup time necessary to establish a nitrifying biofilm was about 3 weeks under low temperature (Uri-Carreño et al., 2021). As reported in Fig. S1, in the early stage of the experiment the electrical conductivity of the influent wastewater was significantly higher than a typical municipal wastewater (< 1mS/cm) because of the high chloride concentration. The reason for this result could be likely due to the infiltration of eddy marine water in the sewage network.

Therefore, it is reasonable that even high concentration of monovalent cations (like Na^+) was present in the wastewater (Le Bonté et al., 2008). The abundance of such elements reduce the flocculating capacity of bacteria, thus slowing the biofilm formation process (Novak et al., 1998).

3.3 Nitrogen removal kinetics in biofilm and suspended biomass

AUR tests were performed on the biofilm attached to the membrane to assess the nitrification kinetics achievable with the MABR technology and the occurrence of simultaneous nitrification and denitrification, as well as on the suspended biomass from the MABR and CAS. Moreover, respirometric batch assays were performed to address the kinetic parameters of the nitrifying bacteria in the suspended biomass. Figure 4 shows the results of the AUR tests performed on the biofilm (Fig. 4a) and on the suspended biomass (Fig. 4b), as well as the main kinetic parameters of nitrifying bacteria (Fig. 4c,d,e). In Figure 4f is reported the comparison between the minimum aerobic SRT to avoid the washout of nitrifying bacteria calculated according to equation 2, and the aerobic SRT imposed in the MABR and CAS.

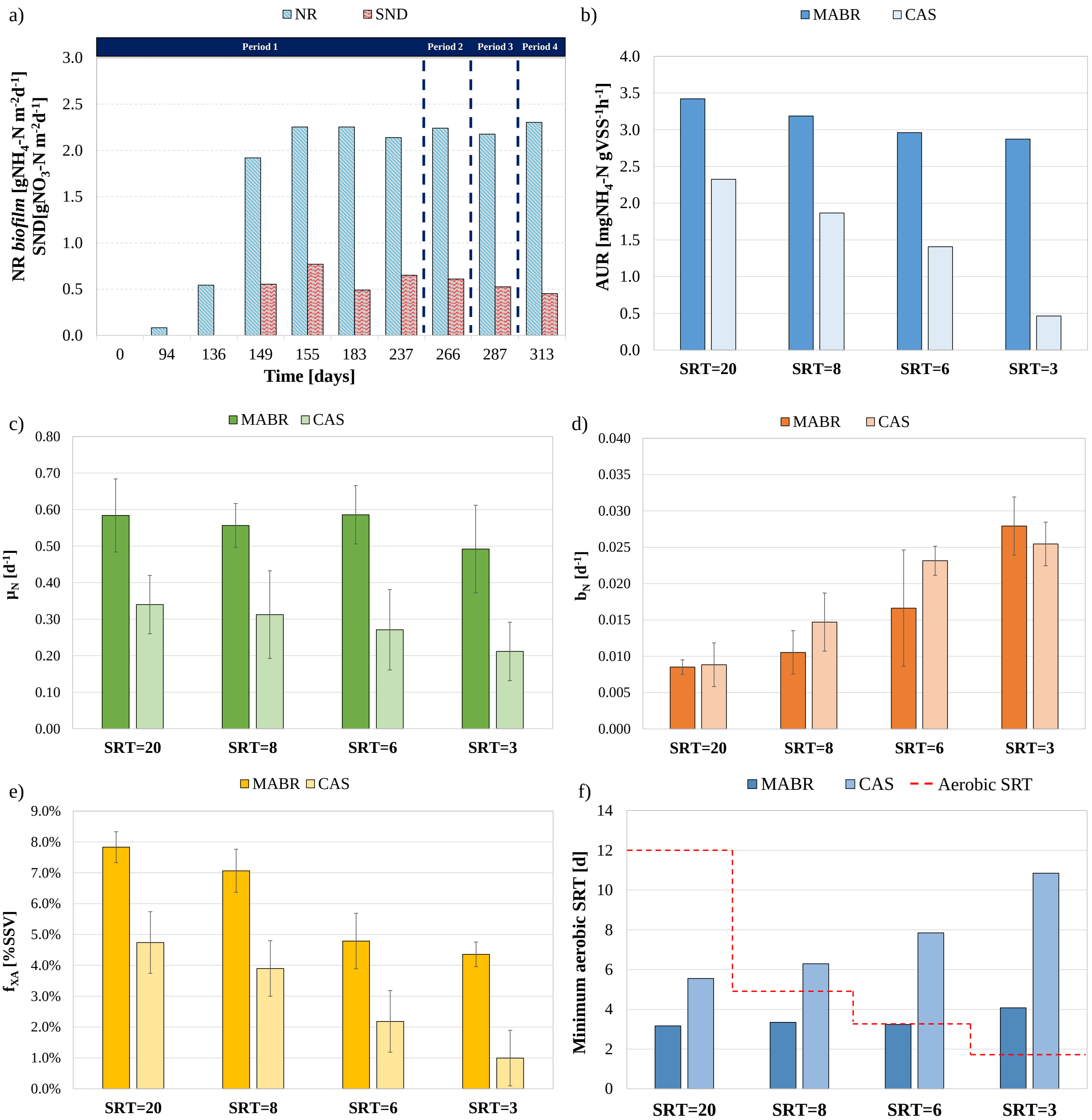

Figure 4: Nitrification (AUR) and simultaneous nitrification-denitrification (SND) rates in the MABR during the experiment (a); steady values of AUR performed in the suspended biomass in MABR and CAS (b); steady values of the maximum growth rate (c), endogenous decay rate (d) and active fraction of nitrifying bacteria (e); comparison between the minimum aerobic SRT and the aerobic SRT in the MABR and CAS.

In Period 1, nitrification activity in the biofilm was observed started from the test performed on the 94nd day, according to the results of mass balance performed on the anoxic tank of the MABR line. Nitrification rate increased during Period 1, reaching a steady value close to 2.30 mgNH_4-N $m^{-2}d^{-1}$ near the 155th day. From this day, simultaneous nitrification and denitrification was observed during the kinetic tests. Indeed, the rate of NH_4-N consumption was higher compared with the NO_3-N production. Because no COD was available during the kinetic tests performed on the biofilm, the ammonium consumed by heterotrophic growth during the test was considered negligible. Consequently, it was concluded that the difference between the rate of NH_4-N consumption and the NO_3-N production was due to the occurrence of simultaneous nitrification and denitrification within the biofilm. Overall, the rate of SND was close to 0.65 mgNO_3-N $m^{-2}d^{-1}$, thereby suggesting that the biofilm thickness was large enough to allow the establishment of an anoxic layer. Nitrification rates observed in this study were comparable with those reported in previous literature operating in a real municipal WWTP (Gilmore et al., 2013; J. Peeters et al., 2017). In contrast, denitrification rate was low because of the availability of endogenous organic substrate only. At steady state in Period 2, Period 3 and Period 4, the nitrification rate of the biofilm was still constant at approximately 2.20 mgNH_4-N $m^{-2}d^{-1}$. Similarly, the SND rate ranged between 0.45 mgNO_3-N $m^{-2}d^{-1}$ and 0.60 mgNO_3-N $m^{-2}d^{-1}$. The above results indicated that the biofilm reached complete maturation and the SRT did not have any effect on the nitrification capacity of the biofilm. Overall, the nitrification rate of the biofilm in the MABR was significantly higher than that reported in other studies on conventional biofilm system. Indeed, Di Trapani and coauthors reported that the biofilm nitrification rate in a MBBR was close to 1 mgNH_4-N $m^{-2}d^{-1}$, thereby almost the half than that observed in this study (Di Trapani et al., 2011). Similarly, in another study carried out on an IFAS-MBR, the average nitrification rate observed in the biofilm was close to 0.85 mgNH_4-N $m^{-2}d^{-1}$ (Mannina et al., 2018). Based on the above, the results obtained in this study demonstrated that the biological activity of the biofilm in a MABR is higher than a conventional biofilm system. The counter-diffusional nature of the biofilm of the MABR allows nitrifying organisms to have additional DO on the inside of the biofilm, thereby creating ideal condition for their growth. In MABR, oxygen is transferred directly from air into the biofilm, so the driving force is greater than what occur in a conventional biofilm process. Because of this, the active part of the biofilm in the MABR is greater than that of a conventional biofilm, thus justifying the higher ammonium removal kinetics.

The AUR of the suspended biomass (Fig. 4b) was determined to evaluate the potential seeding effect of nitrifying biomass derived from the biofilm detachment in the MABR. At the end of Period 1, the average nitrification rate observed in the MABR was close to 3.45 mgNH_4-N gVSS^{-1} h^{-1}, whereas that in the CAS was approximately 2.33 mgNH_4-N gVSS^{-1} h^{-1}. Therefore, the MABR performed a slightly higher nitrification rate compared with the CAS even at high SRT. When decreasing the SRT, the AUR decreased in both the MABR and CAS, although the reduction was much higher in the CAS. Indeed, the AUR in the MABR gradually decreased from 3.45 mgNH_4-N gVSS^{-1} h^{-1} to 2.87 mgNH_4-N gVSS^{-1} h^{-1} when the SRT decreased from 20 days to 3 days, whereas it collapsed from 2.33 mgNH_4-N gVSS^{-1} h^{-1} to less than 0.50 mgNH_4-N gVSS^{-1} h^{-1} in the CAS. This result indicated that a significative washout of nitrifying biomass occurred in the CAS because of the low SRT, thereby confirming the decrease of the nitrification efficiency observed from Period 2. Nevertheless, in the MABR the effect of SRT reduction was little noticeable since the decrease of the AUR accounted for less than 20%. The above results were consistent with previous literature (Di Trapani et al., 2013) and suggested a greater abundance of nitrifying bacteria in the suspended biomass of the MABR deriving from the detachment of the biofilm from the membrane fibers. Therefore, it was demonstrated that the "seeding effect" in an MABR/AS system enables nitrification in the mixed liquor below the washout SRT for conventional activated sludge systems.

The maximum growth rate and the endogenous decay rate of the autotrophic nitrifying bacteria are shown in Figure 4c and 4d, respectively. The μ_N in the MABR was higher than that in the CAS during the entire experiment (p-value < 0.01). In all the four periods, the values of μ_N were approximately twice the ones in the CAS, resulting on average equal to 0.56 d^{-1} and 0.26 d^{-1}, while showing a slightly decreasing tendency with the SRT in both the lines. Similar results were reported in previous literature in hybrid system. Indeed, Mannina et al. observed that the growth rate of the suspended biomass in an integrated fixed film activated sludge membrane bioreactors (IFAS-MBR) was particularly high (much higher compared to the corresponding value of a MBR) (Mannina et al., 2019). Therefore, this result could be likely due to the "seeding" effect of nitrifying bacteria from the biofilm to the mixed liquor that contributed to enrich the activated sludge with autotrophic species.

The endogenous decay rate of nitrifying bacteria increased with the decrease of the SRT in both the lines. Indeed, the b_N increased from 0.009 d^{-1} to approximately 0.028 d^{-1} and 0.026 d^{-1} in the MABR and CAS, respectively. This confirmed that the decrease of the SRT enhanced the decay phenomena that involved the suspended nitrifying biomass. However, statistical analysis did not show a significant difference between the endogenous decay rate in the MABR and CAS sludges.

According to the above results, the active fraction of the autotrophic biomass was higher in the MABR than the CAS (p-value < 0.01). In Period 1, the f_{XA} was close to 8% and 5% in the MABR and CAS, respectively, because the long SRT and the low C/N ratio enabled a significant accumulation of nitrifying biomass within the system. When the SRT decreased, the amount of active fraction reduced because of the washout exerted on the suspended biomass. Indeed, from Period 2 to Period 4, the percentage of the active fraction decreased from 7% to 4.4% in the MABR and from 3.9% and 1% in the CAS, thereby indicating that the washout effect was more intense in the conventional system. Based on the results previous discussed, it is reasonable that the seeding effect increased the amount of the autotrophic active bacteria in the suspended biomass. Therefore, it is possible that the continuous supply of biofilm pieces to the suspended biomass enriched it in nitrifying bacteria enabling to compensate the amount of nitrifying bacteria withdrawn as waste sludge from the suspended sludge.

To further support the above results, it was compared the aerobic SRT imposed in the MABR and CAS with the minimum SRT required for achieving accumulation of nitrifying according to equation 2 (Fig. 4f). In Period 1, the minimum SRTs were 3.16 d and 5.5 d in the MABR and CAS, respectively, thereby resulting lower than the aerobic SRT (12 d) imposed in both the lines. Therefore, no washout occurred during Period 1, thus confirming the high percentage of nitrification observed in this period in both the lines. In Period 2, the minimum SRT in the MABR was similar to that in the previous period, whereas it increased to 6.30 d in the CAS. Consequently, because the aerobic SRT was 4.8 days a partial washout of nitrifying biomass occurred in the CAS, thereby justifying the partial decrease of nitrification performance observed at the end of Period 2. In Period 3, the minimum SRT increased in the CAS to 7.85 days, whereas it was close to 3.2 days in the MABR. Consequently, a significant washout of nitrifying bacteria occurred in the CAS, as demonstrated by the substantial decrease in nitrification performance in Period 3. In contrast, no significant changes occurred in the MABR during Period 3, since the aerobic SRT (3.6 days) was higher than the minimum SRT (3.2 days). Finally, in Period 4 the minimum SRT slightly increased to approximately 4.10 days in the MABR, whereas it arose to 10.85 days in the CAS. Accordingly, a considerable washout of nitrifying bacteria occurred in the CAS, whereas only a partial was noted in the MABR. These results were in accordance with the percentages of nitrogen removal of the experimental pilot plants observed in Period 4. Indeed, in the CAS an almost complete loss in nitrification capacity was observed in Period 4, whereas in the MABR only a partial decrease of nitrification efficiency was noted. The above findings confirmed what previously reported in the literature referring to IFAS system, meaning that all plants implementing a treatment technology based on the coupling between biofilm and suspended biomass are able to operate well below the minimum suspended medium SRT for nitrification in conventional activated sludge systems (Ekama, 2015).

The outcomes from respirometric batch tests demonstrated and confirmed that the transfer of nitrifying organisms from the biofilm to the mixed liquor occurring in the MABR promoted a significant increase of the autotrophic active fraction in the suspended biomass of the MABR and of the main kinetic parameters, in general. Therefore, this enabled to sustain nitrification in the suspended biomass even at SRT lower than the washout SRT of a conventional activated sludge system. It is worth noticing that the present study enabled to discern the ammonium removal kinetic of the biofilm from that of the suspended biomass. In contrast, the previous studies that investigated the kinetics autotrophic bacteria in MABR and IFAS systems for nutrients removal often focused on the suspended biomass activity only, without providing any data for the biofilm activity (Leyva-Díaz et al., 2013). Because of this, it was difficult to compare the results achieved in study with previous literature.

3.4 Performance of oxygen transfer in MABR

To assess the performance of oxygen transfer in the MABR, a daily mass balance was carried out from the online measurement of oxygen concentration in the process and exhaust air. Figure 5 depicts the trends of the OTE and OTR during the experiment.

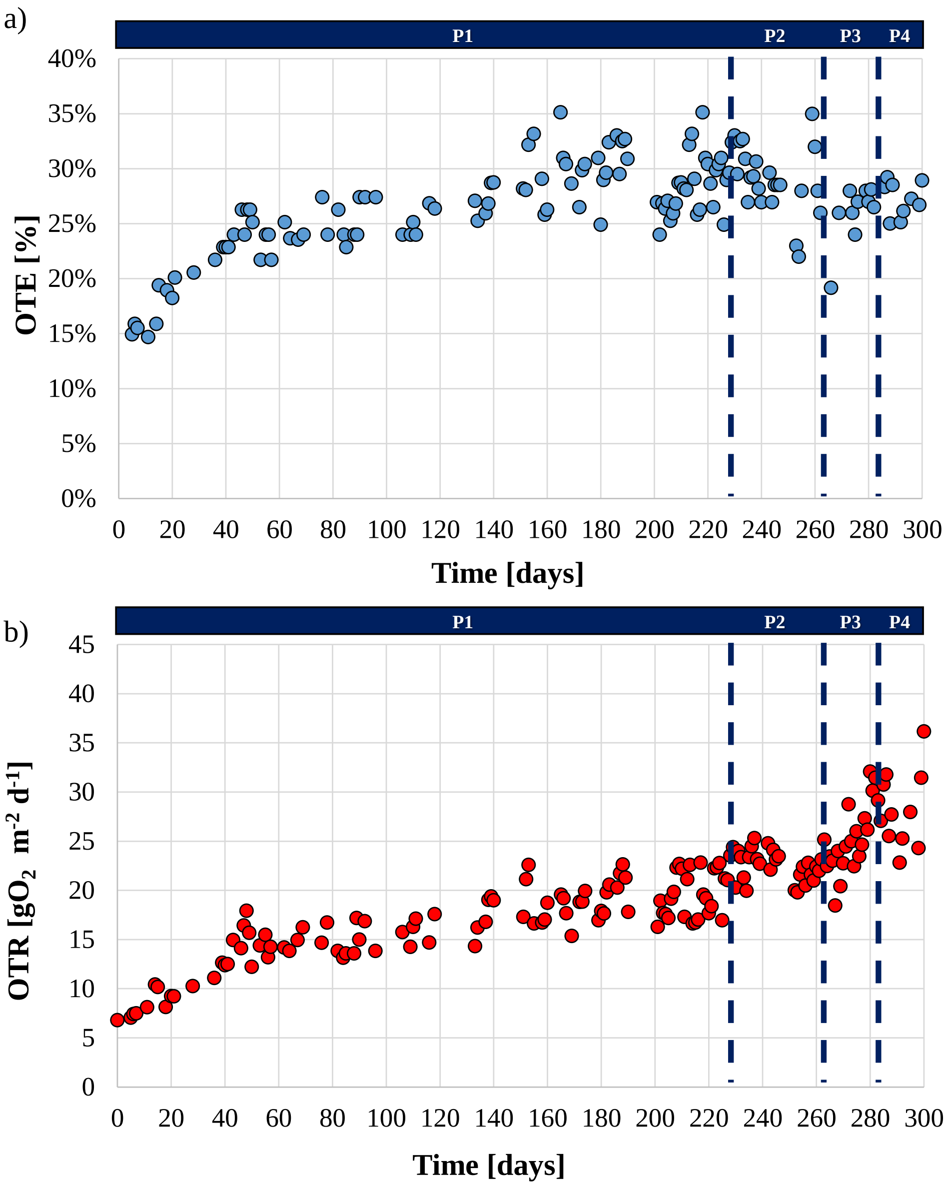

Figure 5: Trend of the daily values for OTE (a) and OTR (b) in the MABR during the experiment

The OTE increased during the start-up phase of the MABR (Fig. 5a). Indeed, during the entire Period 1 and the early of Period 2, the OTE rose from 14% to approximately 25% on the 58th day. The increase of OTE confirmed the occurrence of the biofilm development during this start-up phase, since the percentage of oxygen in the exhaust air was decreasing because of the bacterial consumption. This result was consistent with the nitrification rate observed in the anoxic reactor of the MABR, indicating that a stable biofilm was formed after approximately 60 operational days. Subsequently, the OTE was quite constant at a value close to 30% on average until the end of the

Period 2. In Period 3 and Period 4, the OTE ranged between 26-34%, in good agreement with the change in the total nitrogen concentration in the influent wastewater. Moreover, the OTE did not show any relationship with the decrease of the SRT. Overall, the OTE values were comparable with those reported in other studies (Castrillo et al., 2019; Guglielmi et al., 2020), confirming also that OTE increased during high loading conditions.

The trend of the OTR is reported in Fig. 5b. The OTR increased during the early stage in Period 1 from 5 gO_2 $m^{-2}d^{-1}$ to approximately 22.5 gO_2 $m^{-2}d^{-1}$ consistently with the OTE values and the development of the biofilm on the membrane fibers. Hereafter, the OTR was fairly stable ranging between 15 gO_2 $m^{-2}d^{-1}$ and 22 gO_2 $m^{-2}d^{-1}$ during the rest of the Period 1, with an average value of 16.3 gO_2 $m^{-2}d^{-1}$. In Period 2, Period 3 and Period 4, the OTR showed a constant increasing trend according to the increase of nitrification rate of the biofilm occurred in the same periods. Indeed, the OTR increased to 22.5 gO_2 $m^{-2}d^{-1}$ in Period 2, whereas at the end of Period 3 and Period 4 it reached average values of 26.5 gO_2 $m^{-2}d^{-1}$ and 30.5 gO_2 $m^{-2}d^{-1}$, respectively. The above results indicated that the oxygen transfer rate to the biofilm increased from Period 1 to Period 2, in agreement with the nitrification rate of the biofilm. The achieved result referred to the OTR were slightly higher respect those reported in previous studies (Guglielmi et al., 2020; J. Peeters et al., 2017), likely because of the higher value of the process air delivered to the membrane modules and the higher nitrification rate of the biofilm achieved after Period 3. Nevertheless, the oxygen required for nitrification (resulting from the ratio between the OTR and NR) was close to 5.5 gO_2 gN^{-1} on average, thereby comparable with that obtained in the above-cited studies. This suggested that the oxygen provided to the biofilm was used for nitrification purposes.

3.5 Effect of biofilm detachment on settling properties of the suspended biomass

Biofilm detachment from the membrane might affect the settling properties of suspended biomass in hybrid system. However, no evidence about this is reported in the literature referring to MABR systems. Analysis of particle size distribution on the suspended biomass was regularly performed with the aim to identify the presence of biofilm pieces in the bulk and how this could affect the settling performance of the activated suspended sludge. Figure 6 depicts the cumulative curves of the particle size distribution performed in the suspended activated sludge (Fig. 6a, b), the microscopic images of the activated sludge (100x of magnification) (Fig. 6c, d), the trends of the DSVI (Fig. 5e) and the average values of the EPS in all the experimental periods in the MABR and CAS.

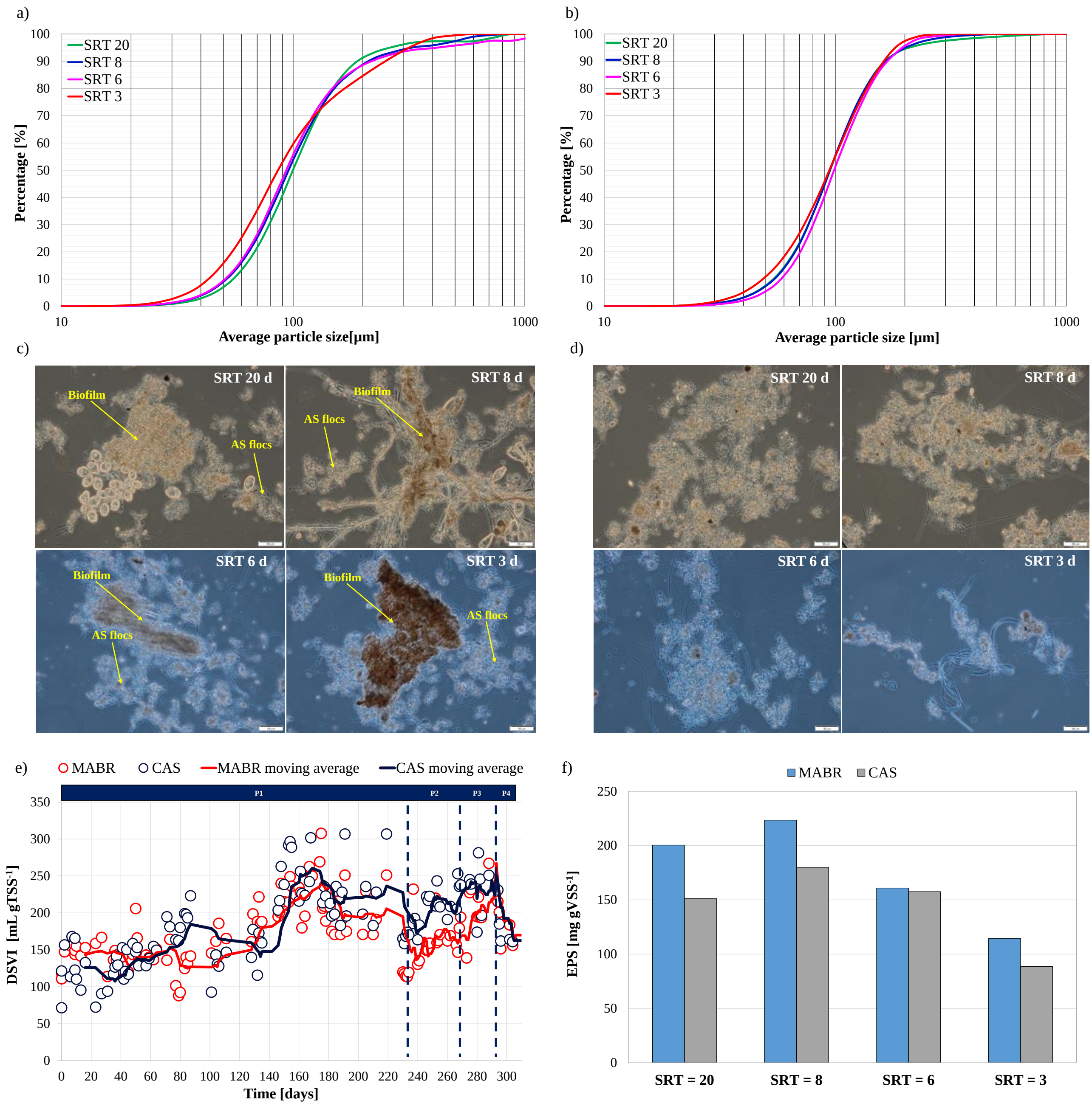

Figure 6: Cumulative particle size distribution of the suspended biomass in the MABR (a) and the CAS (b); microscopic images of suspended sludge samples in the MABR (c) and the CAS (d); trend of the DSVI in the MABR and CAS (e); average specific EPS content in the MABR and CAS (f).

As reported in Figure 6a, the cumulative PSD in the MABR highlighted a significant abundance of particles with a size greater than 200 µm on average. Indeed, in Period 1, the percentage of these particles was close to 9% and this percentage increased in Period 2, Period 3 and Period 4 to approximately 12%, 13 and 16%, respectively, suggesting the presence of pieces of biofilm in the suspended biomass during the entire experiment. In contrast, the above-mentioned percentage was lower than 5% in the CAS during the entire experiment (Fig. 6b), thereby indicating the presence of flocculent biomass only in the suspended sludge. It is worth noticing that in both the process lines, a decrease of the average size of the particles was noted, as suggested by the left-shift of the cumulative PSDs observed with the SRT decreasing.

The presence of biofilm in the bulk of the MABR was also confirmed by microscopic analysis. As shown in Figure 6c, pieces of biofilm were detected as dense and very compact particles, morphologically different respect to activated sludge flocs of the suspended biomass. More precisely, these pieces of biofilm were incorporated within the flocculent sludge, providing a denser and compact structure to the suspended sludge. Moreover, a large presence of attached ciliate protozoa was noted on and inside the biofilm in Period 1 and Period 2, whereas it significantly decreased in the remaining periods of the experiment. These microorganisms typically developed in biofilms at long SRT and their disappearance could be related to the decrease of the sludge age in the system (Huang et al., 2019; Jenkins et al., 2003). Furthermore, the activated sludge flocs of the MABR were denser and more compact respect those of the CAS (Fig. 6d) because of the flocculating effect that the biofilm exerted on the suspended biomass. It is worth noticing that in both the MABR and CAS, the lowering of the SRT caused a decrease of the floc size and their compactness. Indeed, from Period 3, the flocculent sludge exhibited an open structure in which the filamentous organisms led to large, irregularly shaped flocs with substantial internal voids. This was likely related to the relatively young age of the activated sludge flocs in which the maturation stage was not fully achieved. The above results were consistent with previous literature, confirming that short SRT produced flocs with a loose and weak structure (Shao et al., 2020).

The effect of the biofilm pieces on the suspended biomass was clearly visible in terms of settling properties of the activated sludge (Fig. 6e). In general, the settling properties of the activated sludge significantly fluctuated during the entire experiment as a result of the variation of operating parameters (temperature, F/M, C/N) and the wastewater composition in agreement with the literature (Jones and Schuler, 2010). Nevertheless, except for the start-up phase (0-60th day) in which no biofilm on the membrane was observed, the suspended biomass of the MABR showed better and more stable settling properties. After the 60th day, the average value of DSVI was equal to approximately 170 mL $gTSS^{-1}$ and 210 mL $gTSS^{-1}$ on average in the MABR and CAS, respectively. However, when the SRT was decreased to 6 days, the settling performances of the sludge were similar and no significant improvements in the MABR were noted, likely because of the modification in the flocs morphology occurred after the Period 3. The differences observed in the MABR and CAS were statistically significant (*p-value* < 0.01). These results indicated that hybrid configuration of MABR enabled a not negligible improvement of the settling properties of the suspended biomass that, although decreasing with the SRT, involved a decrease of the average value of the DSVI and the achievement of lower variability compared with a conventional activated sludge system. This in turns could imply the choice of lower safety factors in design phase and more stable performances during operations.

The specific EPS content of the suspended biomass was higher in the MABR on average (Fig. 6f). More precisely, in Period 1 and Period 2 the average EPS content in the MABR was close to 210 mgEPS $gVSS^{-1}$, whereas in the CAS it was approximately 165 mgEPS $gVSS^{-1}$. In Period 3 and Period 4, the EPS content significantly decreased in both the MABR and CAS, resulting equal to 150 mgEPS $gVSS^{-1}$ in Period 3 and approximately of 100 mgEPS $gVSS^{-1}$ in Period 4. The decrease of the EPS content of the sludge was consistent with the weakening of the flocs previously discussed. Indeed, it was precisely the EPS reduction that caused the deflocculation of the suspended flocs, since the extracellular polymers play a key role in the formation process of the activated sludge flocs (Wanner, 2017). The differences observed in the four experimental periods were considered statistically significant (*p-value < 0.01*) only during Period 1 and Period 2. Further studies are necessary to investigate the effect of biofilm detachment on the EPS content of the suspended biomass.

Conclusions

A hybrid MABR pilot plant fed with real wastewater was monitored for 304 days. The results achieved in this study demonstrated that the MABR technology enabled to achieve higher performances with reference to TSS, COD and NH_4-N removal, as well as a higher resilience toward the operating parameters variation compared to conventional activated sludge system.

A stable biofilm nitrification rate approximately of 2.40 gNH_4-N $m^{-2}d^{-1}$ was achieved after 150 days, accounting for 25-45% to the overall nitrification observed in the hybrid MABR. The transfer of nitrifying organisms from the biofilm to the mixed liquor occurring in the MABR promoted a significant increase of the autotrophic active fraction in the suspended biomass of the MABR. This enabled to sustain nitrification in the suspended biomass even at SRT lower than the washout SRT of the conventional activated sludge system. Moreover, the seeding effect enabled a not negligible improvement of the settling properties of the suspended biomass in the MABR.

The achieved results confirmed that hybrid MABR could represent a valuable solution for retrofitting existing plants form improving nitrification process and overall performances.

Acknowledgments

Authors warmly thank Suez Group, especially in the persons of Eng. Giuseppe Guglielmi and Eng. Moreno Di Pofi, for providing ZeeLung membrane modules and for their valuable scientific and technical support during the experimental campaign.

The Authors also thank Engg. Francesco Como, Edoardo Simoncini, Matteo Cristofalo and Dario Guida for their fundamental support and contribution provided during the pilot plant operations. Moreover, the authors want to thank AMAP Company for the technical support, Saveco Warmgroup, and George Fisher, for providing the rotating drum screen and hydraulic joints, respectively.
A very special thanks to Prof. David Jenkins recently passed away for his fundamental engagement in the field of biological wastewater treatment and solids separation problems.

References

APHA, 2005. Standard Methods for the Examination of Water & Wastewater, American Public Health Association.

Bryers, J.D., 2018. Modeling biofilm accumulation, in: Physiological Models in Microbiology: Volume II. https://doi.org/10.1201/9781351075640

Bunse, P., Orschler, L., Agrawal, S., Lackner, S., 2020. Membrane aerated biofilm reactors for mainstream partial nitritation/anammox: Experiences using real municipal wastewater. Water Res. X 9, 100066. https://doi.org/10.1016/j.wroa.2020.100066

Capodici, M., Fabio Corsino, S., Di Pippo, F., Di Trapani, D., Torregrossa, M., 2016. An innovative respirometric method to assess the autotrophic active fraction: Application to an alternate oxic-anoxic MBR pilot plant. Chem. Eng. J. 300. https://doi.org/10.1016/j.cej.2016.04.134

Carlson, A.L., He, H., Yang, C., Daigger, G.T., 2021. Comparison of hybrid membrane aerated biofilm reactor (MABR)/suspended growth and conventional biological nutrient removal processes. Water Sci. Technol. 1–11. https://doi.org/10.2166/wst.2021.062

Castrillo, M., Díez-Montero, R., Esteban-García, A.L., Tejero, I., 2019. Mass transfer enhancement and improved nitrification in MABR through specific membrane configuration. Water Res. 152, 1–11. https://doi.org/10.1016/j.watres.2019.01.001

Corsino, S.F., de Oliveira, T.S., Di Trapani, D., Torregrossa, M., Viviani, G., 2020. Simultaneous sludge minimization, biological phosphorous removal and membrane fouling mitigation in a novel plant layout for MBR. J. Environ. Manage. 259, 10986. https://doi.org/10.1016/j.jenvman.2019.109826

Di Trapani, D., Christensso, M., Ødegaard, H., 2011. Hybrid activated sludge/biofilm process for the treatment of municipal wastewater in a cold climate region: A case study. Water Sci. Technol. https://doi.org/10.2166/wst.2011.350

Di Trapani, D., Christensson, M., Torregrossa, M., Viviani, G., Ødegaard, H., 2013. Performance of a hybrid activated sludge/biofilm process for wastewater treatment in a cold climate region: Influence of operating conditions. Biochem. Eng. J. 77, 214–219. https://doi.org/10.1016/j.bej.2013.06.013

Ekama, G.A., 2015. Recent developments in biological nutrient removal. Water SA. https://doi.org/10.4314/wsa.v41i4.11

Gilmore, K.R., Terada, A., Smets, B.F., Love, N.G., Garland, J.L., 2013. Autotrophic nitrogen removal in a membrane-aerated biofilm reactor under continuous aeration: A demonstration. Environ. Eng. Sci. https://doi.org/10.1089/ees.2012.0222

Guglielmi, G., Coutts, D., Houweling, D., Peeters, J., 2020. Full-scale application of mabr technology for upgrading and retrofitting an existing WWTP: Performances and process modelling. Environ. Eng. Manag. J. 19, 1781–1789. https://doi.org/10.30638/eemj.2020.169

Horn, H., Reiff, H., Morgenroth, E., 2003. Simulation of growth and detachment in biofilm systems under defined hydrodynamic conditions. Biotechnol. Bioeng. 81, 607–617. https://doi.org/10.1002/bit.10503

Houweling, D., Long, Z., Peeters, J., Adams, N., Côté, P., Daigger, G., Snowling, S., 2019. Nitrifying below the “washout” SRT: Experimental and modelling results for a hybrid MABR / activated sludge process. 91st Annu. Water Environ. Fed. Tech. Exhib. Conf. WEFTEC 2018 1250–1270. https://doi.org/10.2175/193864718825137944

Hu, H., He, J., Yu, H., Liu, J., Zhang, J., 2017. A strategy to speed up formation and strengthen activity of biofilms at low temperature. RSC Adv. https://doi.org/10.1039/c7ra02223a

Huang, J., Wu, X., Cai, D., Chen, G., Li, D., Yu, Y., Petrik, L.F., Liu, G., 2019. Linking solids retention time to the composition, structure, and hydraulic resistance of biofilms developed on support materials in dynamic membrane bioreactors. J. Memb. Sci. https://doi.org/10.1016/j.memsci.2019.03.033

Jenkins, D., Richard, M.G., Daigger, G.T., 2003. Manual on the Causes and Control of Activated Sludge Bulking, Foaming and Other Solids Separation Problems. IWA, London.

Jones, P.A., Schuler, A.J., 2010. Seasonal variability of biomass density and activated sludge settleability in full-scale wastewater treatment systems. Chem. Eng. J. 164, 16–22. https://doi.org/10.1016/j.cej.2010.07.061

Kinh, C.T., Suenaga, T., Hori, T., Riya, S., Hosomi, M., Smets, B.F., Terada, A., 2017. Counter-diffusion biofilms have lower N2O emissions than co-diffusion biofilms during simultaneous nitrification and denitrification: Insights from depth-profile analysis. Water Res. 124, 363–371. https://doi.org/10.1016/j.watres.2017.07.058

Landes, N., Rahman, A., Morse, A., Jackson, W.A., 2021. Performance of a lab-scale membrane aerated biofilm reactor treating nitrogen dominant space-based wastewater through simultaneous nitrification-denitrification. J. Environ. Chem. Eng. 9, 104644. https://doi.org/10.1016/j.jece.2020.104644

Le Bonté, S., Pons, Marie-Noelle, Potier, O., Rocklin, P., Pons, Marie-Noëlle, 2008. Érudit est un consortium interuniversitaire sans but lucratif composé de l RELATION BETWEEN CONDUCTIVITY AND ION CONTENT IN URBAN WASTEWATER Relation entre conductivité et composition ionique dan les eaux usées urbaines. J. Water Sci. 21, 429–438.

Leyva-Díaz, J.C., Calderón, K., Rodríguez, F.A., González-López, J., Hontoria, E., Poyatos, J.M., 2013. Comparative kinetic study between moving bed biofilm reactor-membrane bioreactor and membrane bioreactor systems and their influence on organic matter and nutrients removal. Biochem. Eng. J. https://doi.org/10.1016/j.bej.2013.04.023

Mannina, G., Capodici, M., Cosenza, A., Di Trapani, D., Ekama, G.A., 2018. The effect of the solids and hydraulic retention time on moving bed membrane bioreactor performance. J. Clean. Prod. 170, 1305–1315. https://doi.org/10.1016/j.jclepro.2017.09.200

Mannina, G., Capodici, M., Cosenza, A., Di Trapani, D., Viviani, G., 2019. The influence of solid retention time on IFAS-MBR systems: analysis of system behavior. Environ. Technol. (United Kingdom) 40, 1840–1852. https://doi.org/10.1080/09593330.2018.1430855

Matsumoto, S., Terada, A., Tsuneda, S., 2007. Modeling of membrane-aerated biofilm: Effects of C/N ratio, biofilm thickness and surface loading of oxygen on feasibility of simultaneous nitrification and denitrification. Biochem. Eng. J. 37, 98–107. https://doi.org/10.1016/j.bej.2007.03.013

Metcalf & Eddy, 2014. Wastewater Engineering: Treatment and Resource Recovery, 5th ed. McGraw-Hill.

Nerenberg, R., 2016a. The membrane-biofilm reactor (MBfR) as a counter-diffusional biofilm process. Curr. Opin. Biotechnol. 38, 131–136. https://doi.org/10.1016/j.copbio.2016.01.015

Nerenberg, R., 2016b. The membrane-biofilm reactor (MBfR) as a counter-diffusional biofilm process. Curr. Opin. Biotechnol. 38, 131–136. https://doi.org/10.1016/j.copbio.2016.01.015

Novak, J.T., Love, N.G., Smith, M.L., Wheeler, E.R., 1998. The effect of cationic salt addition on the settling and dewatering properties of an industrial activated sludge. Water Environ. Res. https://doi.org/10.2175/106143098x123318

Peeters, J., 2016. Innovative Membrane Aerated Biofilm Reactor Technology for Low-Energy Nutrient Removal – Pilot Demonstration.

Peeters, J., Adams, N., Long, Z., Côté, P., Kunetz, T., 2017. Demonstration of innovative MABR low-energy nutrient removal technology at Chicago MWRD. Water Pract. Technol. https://doi.org/10.2166/wpt.2017.096

Peeters, Jeff, Long, Z., Houweling, D., Côté, P., Daigger, G.T., Snowling, S., 2017. Nutrient Removal Intensification with MABR – Developing a Process Model Supported by Piloting. Proc. Water Environ. Fed. 2017, 657–669. https://doi.org/10.2175/193864717821494204

Pronk, M., Bassin, J.P., de Kreuk, M.K., Kleerebezem, R., van Loosdrecht, M.C.M., 2014. Evaluating the main and side effects of high salinity on aerobic granular sludge. Appl. Microbiol. Biotechnol. 98, 1339–48. https://doi.org/10.1007/s00253-013-4912-z

Shao, Y., Liu, G. hua, Wang, Y., Zhang, Y., Wang, H., Qi, L., Xu, X., Wang, J., He, Y., Li, Q., Fan, H., Zhang, J., 2020. Sludge characteristics, system performance and microbial kinetics of ultra-short-SRT activated sludge processes. Environ. Int. https://doi.org/10.1016/j.envint.2020.105973

Syron, E., Semmens, M.J., Casey, E., 2015. Performance analysis of a pilot-scale membrane aerated biofilm reactor for the treatment of landfill leachate. Chem. Eng. J. https://doi.org/10.1016/j.cej.2015.03.043

Uri-Carreño, N., Nielsen, P.H., Gernaey, K. V., Flores-Alsina, X., 2021. Long-term operation assessment of a full-scale membrane-aerated biofilm reactor under Nordic conditions. Sci. Total Environ. 779, 146366. https://doi.org/10.1016/j.scitotenv.2021.146366

Wang, R., Zeng, X., Wang, Y., Yu, T., Lewandowski, Z., 2019. Two-step startup improves pollutant removal in membrane-aerated biofilm reactors treating high-strength nitrogenous wastewater. Environ. Sci. Water Res. Technol. 5, 39–50. https://doi.org/10.1039/c8ew00668g

Wanner, J., 2017. Activated sludge separation problems, in: Activated Sludge Separation Problems. https://doi.org/10.2166/9781780408644_053

Zhang, H., Gong, W., Zeng, W., Chen, R., Lin, D., Li, G., Liang, H., 2021. Bacterial-algae biofilm enhance MABR adapting a wider COD/N ratios wastewater: performance and mechanism. Sci. Total Environ. 146663. https://doi.org/10.1016/j.scitotenv.2021.146663